Mon. Not. R. Astron. Soc. **324**, 343–354 (2001)

Quasars from a complete spectroscopic survey

Martin J. Meyer,[1]★ Michael J. Drinkwater,[1] Steven Phillipps[2] and Warrick J. Couch[3]

[1]*School of Physics, University of Melbourne, Victoria 3010, Australia*
[2]*Department of Physics, University of Bristol, Bristol BS8 1TL*
[3]*School of Physics, University of New South Wales, Sydney 2052, Australia*

Accepted 2000 December 4. Received 2000 December 4; in original form 2000 May 4

ABSTRACT

With the advent of multi-fibre spectrographs such as the 'Two-Degree Field' (2dF) instrument at the Anglo-Australian Telescope, quasar surveys that are free of any pre-selection of candidates and any biases this implies have become possible for the first time. The first of these is that which is being undertaken as part of the Fornax Spectroscopic Survey, a survey of the area around the Fornax Cluster of galaxies, and aims to obtain the spectra of all objects in the magnitude range $16.5 < b_j < 19.7$. To date, 3679 objects in the central π-deg^2 area have been successfully identified from their spectral characteristics. Of these, 71 are found to be quasars, 61 with redshifts $0.3 < z < 2.2$ and 10 with redshifts $z > 2.2$. Using this complete quasar sample, a new determination of quasar number counts is made, enabling an independent check of existing quasars surveys. Cumulative counts per square degree at a magnitude limit of $b_j < 19.5$ are found to be 11.5 ± 2.2 for $0.3 < z < 2.2$, 2.22 ± 0.93 for $z > 2.2$ and 13.7 ± 3.1 for $z > 0.3$.

Given the likely detection of extra quasars in the Fornax survey, we make a more detailed examination of existing quasar selection techniques. First, looking at the use of a stellar criterion, four of the 71 quasars are 'non-stellar' on the basis of the automated plate measuring facility (APM) b_j classification, however inspection shows all are consistent with stellar, but misclassified due to image confusion. Examining the ultraviolet excess and multicolour selection techniques, for the selection criteria investigated, ultraviolet excess would find 69 ± 6 per cent of our $0.3 < z < 2.2$ quasars and only 50^{+14}_{-18} per cent of our $z > 2.2$ quasars, while the completeness level for multicolour selection is found to be 90^{+3}_{-4} per cent for $0.3 < z < 2.2$ quasars and 80^{+14}_{-12} per cent for $z > 2.2$ quasars. The extra quasars detected by our all-object survey thus have unusually red star-like colours, and this appears to be a result of the continuum shape rather than any emission features. An intrinsic dust extinction model may, at least partly, account for the red colours.

Key words: techniques: spectroscopic – surveys – quasars: general.

1 INTRODUCTION

Numerous quasar surveys have been carried out in the past 30 years, gradually improving our knowledge of the number density of these objects and its evolution with cosmic time. As quasars have, by definition, essentially star-like images, a common feature of all these surveys is that they require the selection of some number of potential quasar candidates from among a much larger number of stellar images, in order that their true identity may be confirmed by individual spectroscopy. Such a process, however, inherently biases the survey towards quasars which possess the property used in the pre-selection method, to the exclusion of those that do not (Hewett & Foltz 1994).

For instance, surveys that use variability alone as a pre-selection technique will obviously be biased, in that any quasars not varying in the wavelength or time-scale of the survey will be missed. Because of this, variability is often combined with some other pre-selection technique. Prime amongst these are the ultraviolet excess (UVX) method (e.g. Hawkins & Veron 1995), the use of multi-colour pre-selection (e.g. Koo, Kron & Cudworth 1986), and slitless spectroscopy (e.g. Zitelli et al. 1992). There is, however, no guarantee that non-variable quasars will show ultraviolet excess, nor any other pre-selection property, so that although the use of multiple criteria adds to the chances of achieving completeness, it can not assure it.

Historically, slitless spectroscopy (e.g. with objective prisms) has probably been the most successful technique in locating large numbers of quasars, but there are limitations in the completeness

★ E-mail: mmeyer@physics.unimelb.edu.au

Table 1. Some major quasar surveys.

Survey Name	Reference	Preselection	Mag. Limit
Durham/Anglo-Australian Telescope	Boyle et al. (1990)	UVX	$b < 21.0^a$
2dF QSO Redshift Survey	Boyle et al. (2000)	Multicolour	$18.25 < b_j < 20.85$
Sloan Digital Sky Survey	SDSS web page: www.sdss.org/science/ see also Newberg & Yanny (1997)	Multicolour	$g' \sim 19.7$
Canada France Hawaii Telescope	Crampton, Cowley & Hartwick (1987)	Slitless Spec.	$B < 20.5$
Hawkins & Veron	Hawkins & Veron (1995)	Variability, UVX	$17.5 < B < 21.0$

[a] b_j-magnitude zero pointed on the Johnson B magnitude system.

levels achieved with this method. In particular, slitless spectra generally have low signal to noise ratios and short wavelength ranges, so weak emission line quasars tend to be overlooked and it is possible for a quasar to be missed if none of the characteristic emission lines appear in the waveband observed. Recent examples of slitless spectroscopy surveys include the Large Bright Quasar Survey (LBQS; Hewett, Foltz & Chaffee 1995), Hamburg Quasar Survey (HQS; Hagen et al. 1995) and Hamburg/ESO Survey (HES; Wisotzki et al. 1996), the first two of which provide samples of over 1000 quasars.

Dominating current optical quasar surveys, though, is the use of colour pre-selection techniques. This can be carried out with just two passbands, providing a single colour, as is the case for $U - B$ selected (UVX) surveys such as Durham/Anglo-Australian Telescope (Durham/AAT; Boyle et al. 1990), or can involve as many as six passbands (and hence five independent colours), for example the survey performed by Warren et al. (1991). These techniques rely on the unusual nature of quasar spectra, relative to those of stars, to provide colours sufficiently different from stellar objects. A known limitation of UVX is that it fails to locate many quasars with redshifts greater than $\sim$2, at which point the Lyα line moves from the U- to the B-band, significantly reddening the observed colour and making it indistinguishable from many stars. By using an additional passband, such as R, the above limitation can be avoided as the colour difference present in $U - B$ below $z \sim 2$ will become apparent between the blue and red bands at higher redshifts. Aside from these redshift considerations, the question also remains as to whether all quasars possess spectra that do indeed result in them having unusual, non-stellar-like colours. Current major colour preselected surveys include the 'two-degree Field' (2dF) QSO Redshift Survey (2QZ; Croom et al. 1998; Boyle et al. 2000) and the Sloan Digital Sky Survey (SDSS; SDSS web page: `http://www.sdss.org/science`; see also Newberg & Yanny 1997). Some recent optical quasar surveys and their pre-selection techniques are summarized in Table 1, along with their apparent magnitude limits. As noted earlier, it is possible to combine different selection techniques or surveys. Examples of this approach include Hartwick & Schade (1990) and La Franca & Cristiani (1997). The completeness of various pre-selection methods has been looked at via comparison of different surveys by several authors, most recently by Graham, Clowes & Campusano (1999).

Previously, compiling a quasar catalogue by taking individual spectra for *all* the astrophysical objects in a given region has not been possible because of the time consuming nature of such a task (thus necessitating the use of a pre-selection strategy for locating candidate quasars before spectra are taken, as discussed above). However, the development of a new generation of multi-object spectroscopic systems, exemplified by the 2dF spectrograph on the Anglo-Australian Telescope, now allows us to contemplate such surveys for the first time. Our central aim is to conduct a quasar survey that, as far as possible for a purely optical survey, is *not* biased by the use of a pre-selection technique. For this and other reasons, we have begun observations for the Fornax Spectroscopic Survey project (FSS). To date we have obtained and analysed spectra for essentially all the objects, resolved ('galaxies') and unresolved ('stars'), in a π-deg^2 region of sky in the direction of the Fornax galaxy cluster, within a magnitude range of $16.5 < b_j < 19.7$ (Drinkwater et al. 2000, hereafter Paper I).

In the present paper we discuss, in Section 2, a complete sample of quasars drawn from the FSS data base. Although relatively small, this sample is of importance in that it will provide an independent check on existing surveys and their pre-selection techniques. In Section 3, the data are used to make a new measurement of quasar number counts, comparing this to the major existing optical determinations involving various pre-selection techniques (Boyle et al. 1990 for UVX; Crampton, Cowley & Hartwick 1987 for slitless spectroscopy; Hawkins & Veron 1995 for variability; Boyle et al. 2000 for multicolour). Then, given that more quasars are found than expected from existing surveys, in Section 4 we analyse the U, b_j and R magnitudes available from the survey input catalogue, in order to find out what types of quasars are missed from the UVX (Smith et al. 1997) or multicolour (Croom et al. 1998) pre-selected samples. Finally we examine potential reasons for the unusual colour of these objects. Section 5 provides a summary.

2 DATA

2.1 Observations and reduction

The data for this project are taken from the first field of the 2dF FSS (Paper I). The target list used is a magnitude-limited sample obtained from the Automatic Plate Measuring facility (APM) catalogue of UKST sky survey plates (Irwin, Maddox & McMahon 1994). The epochs of the catalogue plates are 1976 November 18 (b_j) and 1991 September 13 (R). We obtained a more recent U film ourselves on 1997 November 6. Absolute CCD calibrations were obtained for the photographic U, b_j and R magnitudes using the Australian National University 2.3-m telescope in 1999 October. U-band observations, however, were effected by cloud, necessitating the recalibration of these magnitudes on the basis of the Deep Multicolour Survey stellar locus (Osmer et al. 1998). The rms uncertainty in individual photographic magnitudes is 0.13 mag in the U-band, 0.09 mag for b_j and 0.06 mag for R. The 2dF spectroscopic observations in the first π-deg^2 field are over 90 per cent complete in the magnitude range $16.5 < b_j < 19.7$ for both stellar and non-stellar objects. A subsample of slightly fainter stellar objects were also observed as discussed below.

The data were reduced using standard IRAF procedures. No

attempt was made to flux-calibrate the spectra as this is not necessary for the spectral analysis identification processes detailed below. Full details of the FSS survey and its reduction are given in Paper I.

2.2 Redshift and initial type identification

The task of making redshift and initial type identifications from the observed spectra is done as a two step process. In the first step, 10 template spectra are fed into the Image Reduction and Analysis Facility (IRAF) correlation program XCSAO, which cross-correlates the observed spectra with the templates in velocity space (cf. Tonry & Davis 1979). The template and velocity at which maximum correlation occurs is selected as the identification for that object. Of the 10 templates, nine are stellar templates chosen to give a representative sample of star types found in the Milky Way, and one is an emission-line galaxy template. As well as picking up stars in the Milky Way, the first nine templates also pick up absorption-line galaxies. These can be identified as such by noting the velocity determined in the correlation process. Similarly, the emission line galaxy template also picks up a number of different classes of object, correlating strongly with Seyfert 2 galaxies as well as other emission line objects such as starburst and H II galaxies. Identifications of objects for which XCSAO finds a Tonry & Davis correlation parameter of $R < 3.0$ are rejected. The stellar templates used cover a wavelength range of 3500 to 7420 Å, while the emission-line galaxy template covers 3000 to 8000 Å. Spectra are observed in the window 3600–8010 Å.

Following this automatic identification process, all identifications are checked manually, corrections are made and suspected quasars are correlated with a composite quasar spectrum (Francis 1991). Correlation with the quasar template is performed separately to that for the stellar and galactic templates because of the large difference in redshift ranges required for the correlation processes.

2.3 Quasar selection

Although accurately determining object redshifts, the above process does not make unique type identifications. In particular, although all emission line objects will either be correlated with the emission line galaxy or quasar templates, the boundary between quasars and non-quasars within this group is not rigorously defined. To make this distinction, the usual definition of the presence of broad permitted emission lines is used, where broad has been defined as having a measured full width half-maximum $>1100\,\mathrm{km\,s^{-1}}$. Taking into account the resolution of our spectra at $450\,\mathrm{km\,s^{-1}}$, this corresponds to a physical velocity width of $\sim 1000\,\mathrm{km\,s^{-1}}$. One object with an H$\beta$ width greater than this criterion that is not included in the sample is a Seyfert 1.5 with a redshift of 0.22, which is less than the 0.3 lower limit of the survey.

In applying this definition to the 614 objects forming the total group of emission line objects in our field 1, the Hβ line is chosen for measurements as it is visible in the largest number of spectra. The remaining $\sim$60 highest redshift objects have other permitted emission lines measured.

It should be noted here that in defining quasars as all broad line objects, this classification encompasses both objects traditionally defined as quasars as well as objects traditionally defined as Seyfert 1s. If we were to define Seyfert 1s as objects with $M_B > -23$, this would reduce the total quasar sample by $\sim$10 per cent.

From this identification process, of the 3679 objects successfully identified (92 per cent of objects observed), 71 are determined to be quasars, with 61 having redshifts $0.3 < z < 2.2$ and 10 having redshifts $z > 2.2$. The full catalogue of quasars is given in Table 2 which lists their positions, b_j-magnitude, $U - b_j$ and $b_j - R$ colours, absolute blue magnitudes, blue dust extinction values, APM b_j classification and redshifts. Absolute magnitudes were calculated assuming a standard $\Omega_0 = 1$, $\Lambda_0 = 0$ cosmology with $H_0 = 50\,\mathrm{km\,s^{-1}\,Mpc^{-1}}$. We assume a k-correction appropriate for a power law spectrum of slope $\alpha = -0.5$, i.e. $k(z) = -1.25\log(1+z)$. In the APM b_j-band, the extinction due to dust is given by $A_{b_j} = 4.035E(B-V)$, where the values of $E(B-V)$ can be determined from the dust maps of Schlegel, Finkbeiner & Davis (1998). Spectra of all the quasars are shown in the Appendix.

Comparing the quasar identifications to those previously known to exist in the field, four of the six quasars from the Hewitt & Burbidge (1993) catalogue are re-identified. Of the two non-reidentified quasars, the first (0335−353, $z = 1.002$, $b_j = 19.21$, $M_{b_j} = -25.03$) was observed under cloudy conditions and its spectrum was not of sufficient quality to enable identification. Corrections are made for such objects, however, as detailed in the next section. The other non-reidentified quasar (0335−350, $z = 0.321$, $b_j = 18.96$, $M_{b_j} = -22.61$) had a redshift determined in agreement with the existing value, however the spectrum of the object was not good enough to detect any broad Hβ emission, and as such was not classified as a quasar.

3 SURFACE DENSITY OF QUASARS

3.1 Number count measurements

Although the survey technique used in this work is such that ideally no correction is needed for unobserved objects, observational constraints necessitate some consideration of this issue. In particular, due to causes such as faulty fibres and incorrect fibre placements, there is some incompleteness in the successful identification of APM catalogue objects in the range $16.5 < b_j < 19.7$. Also, because of a number of objects being observed beyond the faint end of this range (faintest at $b_j = 20.5$), a correction is needed if we wish to make use of this data, as it is significantly incomplete.

The observational incompleteness correction factor is just the ratio of the number of input catalogue objects of an appropriate type to the number of those objects successfully observed and spectroscopically identified. In particular, this is restricted to stellar objects in the input list as all but four of the 71 identified quasars are classified as stellar in the b_j-band in the APM catalogue. The colour range of objects used is also restricted to $-0.4 < b_j - R < 0.8$, corresponding to the colour range of the actually identified quasars (Fig. 1a). Applying these classification and colour restrictions, histograms of input catalogue and successfully identified objects are plotted Fig. 1(b). These are then cumulated and finally the correction factor as a function of magnitude is determined by taking the ratio of these (Fig. 1c). All correction factors for magnitudes less than 18 are set to unity, with only one quasar observed brighter than this limit.

Using this correction process, adjustments for two classes of object are in fact being made, first, for objects that were simply unobserved, and secondly, for objects that were observed but

Table 2. Quasar catalogue.

No.	RA (J2000)	Dec	b_j (mag)[a]	$U-b_j$ (mag)[a]	b_j-R (mag)[a]	M_{b_j} (mag)[b]	Dust (mag)[c]	APM Class.[d]	z[e]
1	03 42 35.64	−35 58 56.0	19.03	−0.23	0.31	−22.30	0.05	−1	0.309
2	03 39 44.07	−34 41 30.9	19.75	−1.20	0.99	−21.65	0.04	−1	0.318
3	03 37 29.03	−35 41 8.8	18.84	−0.24	0.27	−22.93	0.05	2	0.388
4	03 33 50.74	−35 33 27.8	19.49	−0.28	0.54	−22.46	0.05	−1	0.409
5	03 37 3.57	−35 41 14.0	19.67	0.40	0.54	−22.56	0.05	−1	0.468
6	03 37 36.68	−35 33 35.9	18.84	−1.13	0.78	−23.40	0.06	−1	0.469
7	03 37 39.71	−35 34 18.2	19.43	−0.74	0.15	−22.82	0.06	−1	0.471
8	03 41 42.44	−35 14 8.4	19.19	0.09	−0.35	−23.29	0.04	−1	0.525
9	03 39 7.47	−34 50 59.3	19.81	−0.65	0.32	−22.86	0.05	−1	0.572
10	03 38 53.04	−34 37 54.4	19.42	−0.76	0.21	−23.38	0.04	−1	0.610
11	03 36 50.72	−35 42 40.5	18.79	0.25	0.00	−24.29	0.05	−1	0.696
12	03 41 44.27	−35 44 32.8	19.87	−0.03	0.06	−23.25	0.04	−1	0.709
13	03 38 43.59	−35 33 49.5	19.64	−0.41	0.23	−23.41	0.05	1	0.741
14	03 37 45.74	−34 40 12.5	19.68	−1.10	0.67	−23.57	0.05	−1	0.753
15	03 35 4.65	−35 45 23.7	20.07	−0.13	0.00	−23.19	0.06	−1	0.758
16	03 35 14.13	−35 31 40.6	19.61	−0.07	0.06	−23.81	0.06	−1	0.815
17	03 42 54.70	−35 12 39.0	19.78	0.60	0.17	−23.66	0.04	−1	0.822
18	03 36 21.15	−35 33 35.3	19.92	0.33	−0.15	−23.57	0.05	−1	0.845
19	03 37 37.53	−35 00 3.9	19.62	−0.40	0.56	−23.90	0.06	−1	0.854
20	03 40 15.48	−35 28 50.2	18.96	−1.01	−0.02	−24.57	0.04	−1	0.855
21	03 39 42.94	−35 24 10.4	19.68	−1.19	0.70	−24.27	0.06	−1	1.043
22	03 41 48.45	−36 04 2.7	18.73	−0.10	−0.24	−25.23	0.04	−1	1.049
23	03 36 9.33	−36 07 32.8	18.13	−0.89	0.46	−25.92	0.04	−1	1.093
24	03 40 43.63	−35 47 17.3	19.33	−0.88	0.48	−24.73	0.04	−1	1.100
25	03 40 31.17	−35 05 9.7	19.73	−0.43	−0.05	−24.48	0.05	−1	1.178
26	03 41 6.64	−36 08 42.5	20.00	−1.16	0.91	−24.24	0.04	−1	1.199
27	03 34 32.48	−35 41 9.1	19.28	−1.08	0.37	−25.01	0.06	−1	1.227
28	03 42 21.89	−34 55 27.2	18.89	−0.75	0.69	−25.47	0.04	−1	1.268
29	03 36 27.78	−35 55 49.5	19.33	−0.79	0.56	−25.09	0.05	−1	1.305
30	03 39 47.34	−35 42 41.7	19.71	0.07	−0.37	−24.79	0.04	−1	1.353
31	03 39 27.51	−34 37 7.1	19.68	−0.10	0.63	−24.83	0.05	−1	1.364
32	03 40 23.03	−35 16 7.0	18.92	−0.73	0.34	−25.60	0.05	−1	1.368
33	03 39 58.49	−34 45 54.9	19.11	−0.73	0.01	−25.53	0.04	−1	1.445
34	03 37 1.68	−35 08 8.2	19.31	−0.27	0.04	−25.41	0.07	−1	1.509
35	03 37 55.03	−35 48 20.7	19.65	−1.20	0.06	−25.08	0.04	−1	1.511
36	03 36 54.05	−36 16 6.6	18.61	−0.42	0.41	−26.07	0.05	2	1.541
37	03 36 45.87	−35 42 30.0	20.50	−0.91	1.23	−24.31	0.05	−1	1.569
38	03 39 35.15	−35 55 32.4	19.86	−1.22	0.35	−24.99	0.05	−1	1.601
39	03 37 36.72	−35 14 44.0	19.80	−0.95	0.57	−25.06	0.06	−1	1.608
40	03 39 51.38	−35 55 16.3	19.24	−0.76	0.34	−25.62	0.05	−1	1.612
41	03 42 52.21	−35 28 17.3	19.45	−0.49	0.00	−25.42	0.05	−1	1.619
42	03 40 17.51	−36 03 12.3	19.67	0.06	−0.61	−25.23	0.05	−1	1.638
43	03 39 23.91	−36 04 47.9	18.92	−0.59	−0.10	−26.02	0.05	−1	1.668
44	03 42 28.33	−35 04 44.4	18.97	−0.51	0.18	−25.97	0.04	−1	1.673
45	03 34 13.33	−35 29 57.2	18.86	−0.66	0.30	−26.12	0.06	−1	1.703
46	03 39 30.64	−35 48 47.2	18.82	−0.52	−0.14	−26.17	0.05	−1	1.716
47	03 34 21.08	−35 18 38.9	19.88	−1.13	0.27	−25.21	0.06	−1	1.803
48	03 36 16.95	−34 38 52.7	20.00	−0.43	–	−25.12	0.05	−1	1.819
49	03 37 2.42	−35 36 39.5	19.82	−0.40	−0.03	−25.32	0.05	−1	1.841
50	03 36 37.16	−35 04 32.2	19.72	−0.68	0.20	−25.44	0.07	−1	1.859
51	03 42 56.45	−35 13 15.3	19.39	−0.72	0.17	−25.82	0.04	−1	1.898
52	03 39 6.83	−35 54 21.3	19.93	−1.08	0.32	−25.32	0.05	−1	1.940
53	03 40 19.24	−35 46 18.8	19.87	−0.90	0.33	−25.41	0.03	−1	1.961
54	03 35 53.62	−35 49 24.1	18.53	−1.08	0.26	−26.78	0.04	−1	1.990
55	03 38 46.92	−35 47 17.6	17.26	−0.43	−0.27	−26.72	0.05	2	2.007
56	03 37 37.37	−36 06 4.8	18.59	−1.20	0.41	−26.74	0.05	−1	2.016
57	03 36 10.23	−36 04 3.6	18.81	−0.51	0.08	−26.53	0.04	−1	2.024
58	03 41 3.22	−36 10 11.2	20.03	0.12	0.44	−25.42	0.04	−1	2.131
59	03 42 31.40	−35 47 41.5	19.90	−0.18	−0.24	−25.58	0.04	−1	2.165
60	03 40 20.06	−36 11 16.5	19.06	−0.56	0.35	−26.44	0.05	−1	2.189
61	03 40 6.26	−35 56 25.1	19.72	−0.06	0.30	−25.78	0.05	−1	2.191
62	03 35 24.41	−35 48 1.0	19.91	−0.34	0.18	−25.64	0.05	−1	2.244
63	03 42 11.76	−34 54 6.2	19.30	−0.56	−0.09	−26.26	0.04	−1	2.258
64	03 35 43.05	−35 24 2.6	20.11	0.26	–	−25.57	0.05	−1	2.386
65	03 36 9.04	−34 55 11.3	18.33	−0.42	0.03	−27.37	0.06	−1	2.408
66	03 38 11.87	−36 12 33.0	19.50	−0.11	−0.05	−26.21	0.05	−1	2.420
67	03 41 2.10	−35 20 34.5	19.38	−0.26	0.58	−26.33	0.05	−1	2.426
68	03 42 24.04	−35 08 50.7	19.30	−0.14	0.38	−26.44	0.04	−1	2.456
69	03 37 52.18	−35 58 18.7	19.85	−0.40	0.36	−25.93	0.05	−1	2.509

Table 2 – *continued*

No.	RA (J2000)	Dec	b_j (mag)[a]	$U-b_j$ (mag)[a]	b_j-R (mag)[a]	M_{b_j} (mag)[b]	Dust (mag)[c]	APM Class.[d]	z[e]
70	03 41 46.81	−35 25 28.9	19.13	−0.98	0.54	−26.72	0.04	−1	2.594
71	03 36 1.56	−35 54 23.1	19.71	−0.39	0.36	−26.55	0.05	−1	3.173

[a] Re-calibrated APM magnitudes (see Section 2.1), not corrected for dust extinction.
[b] Absolute magnitude.
[c] Extinction in the b_j band as a result of dust in the Milky Way as determined from the maps of Schlegel, Finkbeiner & Davis (1998).
[d] APM b_j classification: −1, star; 0, noise; 1, galaxy; 2, merged.
[e] Redshift determined from template correlation process (see Section 2.2). Errors are ±0.001.

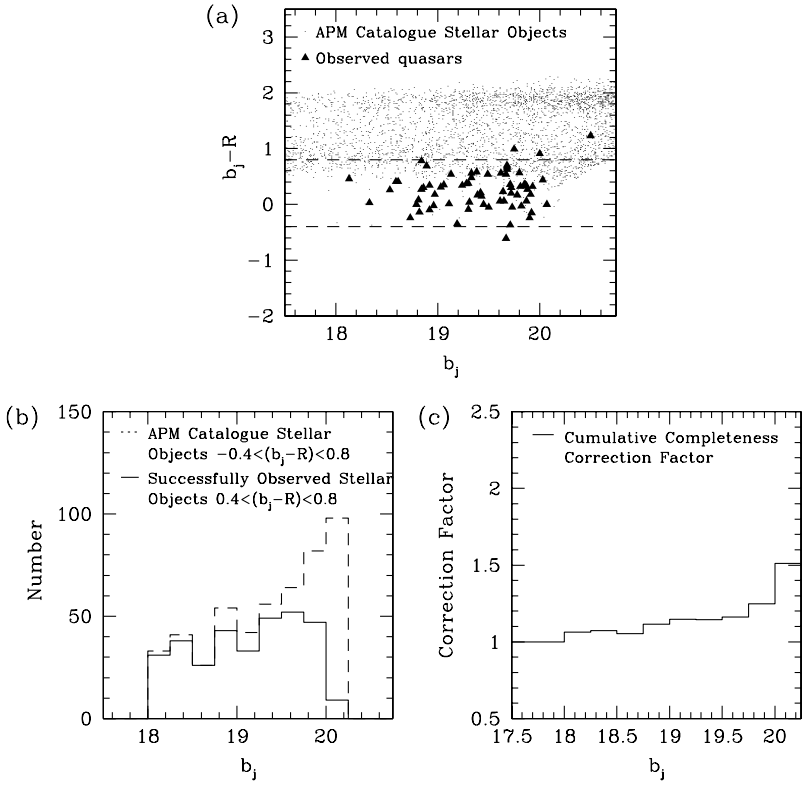

Figure 1. The observational completeness correction factor for quasar number counts: (a) colour range over which determination made; (b) comparison of catalogue versus successfully observed stellar objects; (c) resultant correction factor to observed cumulative quasar number counts – defined as the ratio of catalogue stellar object to successfully observed stellar object integral counts.

whose spectra are not of sufficient quality to enable identification. A potential biasing effect in correcting for the second class of object is the possibility that in poor spectra quasars are easier to identify than other astrophysical objects. To place limits on the size of this effect, for the worst case scenario in which none of unidentified objects were quasars, the overestimate of quasar number counts would be 9 per cent (still less than Poisson errors). However, weak-lined quasars would not be identified in these poor spectra – as shown by one example (see Section 2.3), so the effect is likely much smaller and we do not make a correction for its effects here.

Quasar number counts can also be affected by extinction caused by foreground dust in the Galaxy. To correct for this, quasar b_j mag are adjusted in the number count determinations by the appropriate extinction values as determined in Section 2.3.

Applying the determined correction factors, the integrated quasar number counts per square degree can be obtained, viz.

$$n_{\rm corr} = N_{\rm obs}\,\frac{C_{\rm unobs}}{\rm Area} \qquad (1)$$

where $n_{\rm corr}$ is the corrected number density, $N_{\rm obs}$ is the observed number and $C_{\rm unobs}$ is the correction factor due to unobserved objects and Area is the area of the sky measured, corrected for the presence of bright galaxies. Fractional errors will be of order $\Delta n_{\rm corr}/n_{\rm corr} = 1/\sqrt{N_{\rm obs}}$. Compared to this Poisson uncertainty, the error in the effective area of the field due to other images (primarily bright Fornax Cluster galaxies) and the error in $C_{\rm unobs}$ are negligible, as is the expected effect on the numbers due to quasar clustering on the angular scale of the survey (Boyle et al. 1999). The resultant number counts are plotted in Figs 2 and 3 and given numerically in Table 3. Low z differential counts are given in Fig. 4. These are, we believe, the first such determinations using

a complete all-object spectroscopic technique such as employed in our survey. The data are divided into high ($z > 2.2$) and low ($0.3 < z < 2.2$) redshift bins, the boundary corresponding to the effective limit of the UVX technique. The uncorrected number counts are also given to display the effects of the corrections made.

3.2 Error analysis

Before comparing with other surveys, some possible distorting factors should be assessed. Consider first gravitational lensing. The region surveyed is not a random patch of sky, but rather one intersected by the Fornax Cluster itself at $z = 0.004$ and a recently discovered background cluster at $z = 0.11$ (Hilker et al. 1999). The background cluster at $z = 0.11$ is very closely aligned with Fornax, the brightest galaxies of each having a separation of only 1.1 arcmin. Nevertheless, the projected mass densities of these clusters should be too small to cause any significant lensing, Fornax, in particular, being far too close to us relative to the expected quasars for gravitational lensing to occur.

As a final check that none of the clusters are causing any unusual number count effects through lensing, or for that matter through any other radially dependent effects such as dust extinction, the radial distribution of quasars can be compared to that expected for a random distribution using a Kolmogorov–Smirnov test. The two distributions are found to differ only at the 66 per cent confidence level, i.e. there is no evidence that the distribution of quasars is non-uniform.

As a point of interest, the observed quasars were also checked individually to see if any could be gravitationally lensed pairs caused by a single massive galaxy. Even the three closest pairs are too far apart to be macro-lensed images, each having a separation of ~1 arcmin. The redshifts of the pair closest to the centre of the field are in fact very similar, potentially indicating large scale structure at this location. The spatial separation and relative velocity of these objects are 390 kpc and 286 km s^{-1} respectively, for our assumed cosmology. It should also be noted here that the spectra of these two objects are quite distinct, as can be seen by inspecting the spectra of objects 6 and 7 in the appendix.

The final potential influence on quasar number counts to be considered is the effect of the Eddington bias: because there are more objects of a particular type observable in a fainter magnitude

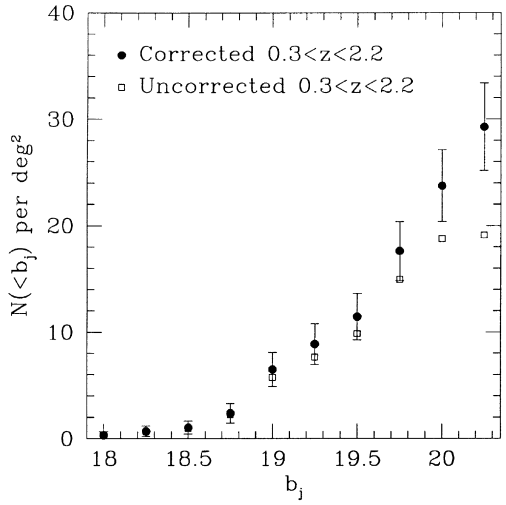

Figure 2. Cumulative low-redshift quasar number counts corrected for observational incompleteness.

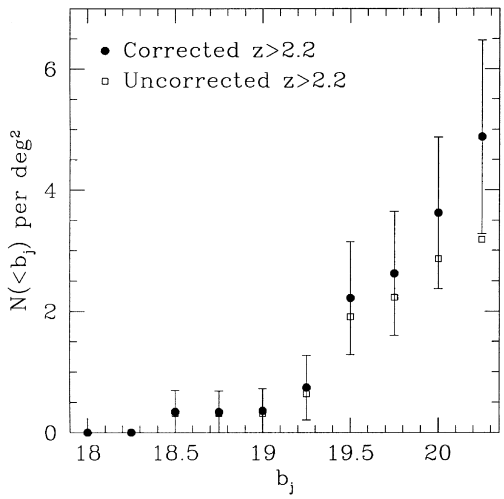

Figure 3. Cumulative high-redshift quasar number counts corrected for observational incompleteness.

Table 3. Quasar number counts.

b_j Mag. Limit (mag)	Cumulative Number Counts[a] $0.3 < z < 2.2$ N^b	Uncorrected ($\deg^{-2}$)	Corrected ($\deg^{-2}$)	Error ($\deg^{-2}$)	Cumulative Number Counts[a] $z > 2.2$ N^b	Uncorrected ($\deg^{-2}$)	Corrected ($\deg^{-2}$)	Error ($\deg^{-2}$)
17.50	1	0.32	0.32	0.33	0	–	–	–
17.75	1	0.32	0.32	0.33	0	–	–	–
18.00	1	0.32	0.32	0.33	0	–	–	–
18.25	2	0.64	0.69	0.49	0	–	–	–
18.50	3	0.95	1.04	0.61	1	0.32	0.35	0.35
18.75	7	2.23	2.38	0.93	1	0.32	0.34	0.34
19.00	18	5.7	6.5	1.6	1	0.32	0.36	0.36
19.25	24	7.6	8.9	1.9	2	0.64	0.74	0.53
19.50	31	9.9	11.5	2.2	6	1.91	2.22	0.93
19.75	47	15.0	17.6	2.8	7	2.2	2.6	1.0
20.00	59	18.8	23.8	3.4	9	2.9	3.6	1.2
20.25	60	19.1	29.3	4.1	10	3.2	4.9	1.6

[a] Number brighter than specified magnitude limit.
[b] Quasars are defined as broad emission-line objects, where broad is taken as having a measured full width half-maximum >1100 km s^{-1}. The survey area is π deg^2. Quasar b_j magnitudes are corrected for dust extinction in determining number counts.

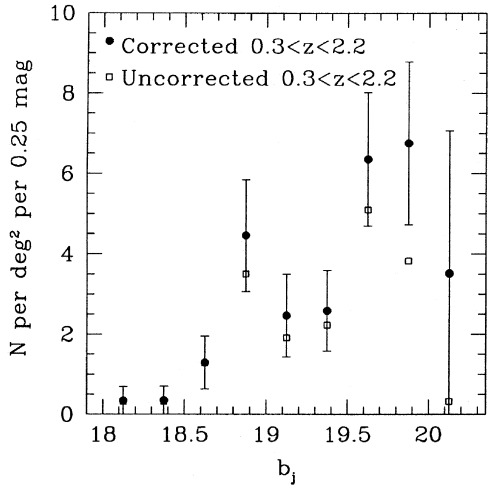

Figure 4. Differential low-redshift quasar number counts corrected for observational incompleteness.

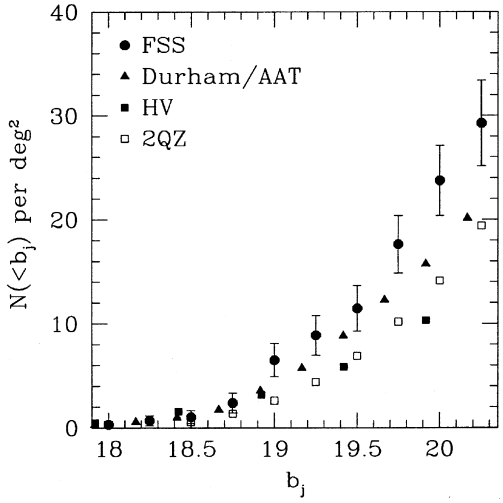

Figure 5. Number count comparisons with existing surveys, $z < 2.2$: Durham/AAT (Durham/Anglo Australian Telescope, Boyle et al. 1990); HV (Hawkins & Veron 1995); 2QZ (2dF Quasar Redshift Survey, Boyle et al. 2000).

bin than in a brighter one, random magnitude measurement errors result in more fainter objects being scattered into the brighter magnitude bin than vice versa. For the survey at hand, the magnitude error is of the order $\sigma \sim 0.1$, implying an overestimate in number counts of only ~2 per cent (Hartwick & Schade 1990). Given the small size of this effect it is ignored in our number count determinations (as, also, in the surveys with which the Fornax data will be compared). Clearly statistical $\sqrt{N}$ errors dominate over all other uncertainties for the present small sample.

3.3 Comparison with number counts in recent surveys

In comparing the number counts of this survey with existing data, a major survey utilizing each of the traditional optical pre-selection techniques is chosen, as discussed in Section 1. It should be noted that these do not all span exactly the same magnitude or redshift range as covered by this survey, but the available data are plotted as applicable. For surveys other than 2QZ, a conversion is made between B magnitudes and b_j mag using the relation $b_j = B - 0.28(B - V)$, and assuming an average quasar colour of $B - V = 0.3$ (Boyle et al. 1990). In making comparisons with existing surveys, of most statistical significance are the low-redshift number counts and the combined high- and low-redshift sample. With ten quasars in the high redshift bin, the numbers are simply too small to make any statistically robust conclusions. In terms of quasar definitions used in each survey, no distinction between Seyfert 1s and quasars is made by any of the Durham/AAT, 2QZ, HV or CFHT surveys, the HV and CFHT samples also including Seyfert 2s.

The comparative number count plots are given in Figs 5 and 6. It can be seen that the Fornax results are higher than the other surveys under consideration, as expected given the complete observation strategy employed. Taking a straight ratio of the Fornax cumulative number counts to those of other surveys, the following $z < 2.2$ ratios are determined at a limit of $b_j = 19.42$ ($B = 19.50$; errors entirely from Fornax): Durham/AAT – 1.27 ± 0.25; HV – 1.92 ± 0.37; and interpolating the CFHT result yields a ratio of 0.99 ± 0.19. Initial results from 2QZ give a surface density of 6.87 ± 0.19 at a magnitude limit of $b_j = 19.5$ (Croom, private communication). Comparing this to the Fornax results gives a ratio of 1.67 ± 0.32.

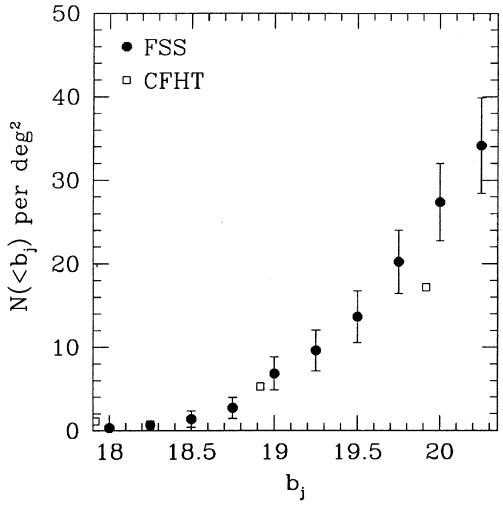

Figure 6. Number count comparisons with existing surveys, all z: CFHT (Canada–France–Hawaii Telescope, Crampton, Cowley & Hartwick 1997).

This comparison suggests that the highest levels of completeness are obtained in the CFHT slitless spectroscopy catalogue, while, probably as expected, low levels of completeness obtain in the HV variability survey (c.f. Hook et al. 1994). Also of interest is the higher level of completeness, i.e. in number counts, of the Durham/AAT survey with respect to the 2QZ at these magnitudes, a point that will be returned to in Section 4.3.

However, the number count comparisons are only *indicative* of survey completeness: because of our low total number of quasars, our counts are no more than ~2-sigma greater than the other surveys examined (except HV at 2.5-sigma). A more direct way to look at the effectiveness of traditional methods is to determine which, if any, of the quasars in our present sample would not have been selected by the traditional colour pre-selection techniques.

4 EFFECTIVENESS OF TRADITIONAL COLOUR PRE-SELECTION

Given the above comparisons with traditional samples, we may suspect that a number of quasars are being overlooked by the pre-selection techniques used. To see which kind of quasars have been found in the present survey that others might miss we examine, first, the stellar nature of the Fornax quasars. We then use the U, b_j and R magnitudes available from the APM survey input catalogue to analyse the UVX criteria initially proposed by Smith et al. (1997) for the 2QZ and the multicolour Ub_jR technique currently being employed by the survey (Croom et al. 1998).

4.1 Non-stellar classified quasars

Of the 71 quasars in the Fornax sample, four are identified in the APM catalogue as being non-stellar in the b_j band. All of these in fact have redshifts $z < 2.2$, meaning that in this redshift range, non-stellar classified objects constitute 7 per cent of the Fornax population. For surveys generating input catalogues purely on the basis of stellar classified objects, such as the UVX and multicolour techniques to be examined here, this incompleteness needs to be considered in addition to the incompleteness caused through the use of the colour pre-selection technique. Looking at the plate images of the non-stellar classified objects, none of the four objects appears to be actually extended, in three cases the extended classification being due the close proximity of a star or galaxy along the line of sight.

4.2 Ultraviolet excess

Plotted in Fig. 7 are all the objects classed as stellar in our catalogue of successfully identified objects, as well as the identified quasars, broken into high- ($z > 2.2$) and low-redshift ($0.3 < z < 2.2$) samples. The dashed line drawn here is the UVX cut-off used by Smith et al. (1997) for selecting candidate objects for the 2QZ and is similar to those of other UVX selected samples (e.g. Boyle et al. 1990; see also La Franca & Cristiani 1997). Although this criterion was never actually used to conduct the survey (being supplanted by the multicolour criterion analysed in the following sub-section when R-band magnitudes became available), extensive work was done on its validity using current data (Croom 1997; Smith et al. 1997; Smith 1998). From Fig. 7 it is clear that using such a criterion will, indeed, result in significant survey incompleteness, with 19 out of the 61 low-redshift quasars not being selected (69 per cent completeness), and five out of the 10 high-redshift quasars (50 per cent completeness). A bootstrapping technique was used to determine errors for these completeness levels. In this, pseudo-samples were generated by selecting quasars at random from the observed population, allowing repetition. A completeness distribution was then determined by applying the UVX criterion to each of the samples, the standard deviation of the upper and lower portions of this distribution from its mean giving upper and lower errors on the original completeness measurement. This gives a completeness range of 69 ± 6 per cent for low-redshift quasars and 50^{+14}_{-18} per cent at higher redshifts.

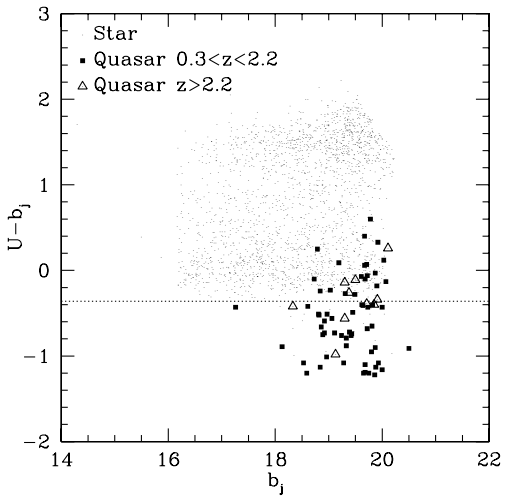

Figure 7. UVX diagram showing colour pre-selection cut-off as initially proposed for use in the 2QZ. Cut-off is located at $U - b_j < -0.36$.

To assess the degree to which our photometric errors may be causing an offset in the derived completeness levels due to the quasar population being skewed towards the blue around the cut-off applied, the same bootstrapping was done adding a random Gaussian error to the colour of each object based on the RMS photometric errors (0.13 mag in U, 0.09 mag in b_j). For this the average completeness value for the generated samples was lower than that of the observed population by 4 per cent for low-redshift and 6 per cent for high-redshift quasars. A UVX survey conducted with zero photometric errors could therefore expect to obtain completeness values higher by similar offsets.

Comparing these results to the predicted 2QZ completenesses for $0.3 < z < 2.2$ objects using this technique, our results are just overlapping with those for the southern field at 78 ± 6 per cent (Croom 1997), but do not encompass the 85 ± 6 per cent for the equatorial field (Smith 1998). In considering the effectiveness of UVX selection, our results are consistent with those of Graham et al. (1999).

4.3 Multicolour

Plotting the same set of objects, except this time on a Ub_jR multicolour diagram (Fig. 8) with the pre-selection criteria currently in use by the 2QZ (Croom et al. 1998), it can be seen that this pre-selection technique *is* much more successful than $U - b_j$ colour alone. Again dividing the Fornax sample into two redshift bins, only six out of the 61 low-redshift quasars are not selected this time (90 per cent completeness), and just two of the 10 high-redshift quasars (80 per cent completeness). Assessing errors as before gives a completeness range of 90^{+3}_{-4} per cent for low-redshift quasars and 80^{+14}_{-12} per cent at higher redshifts.

Adding in Gaussian errors to the quasar colours as before results is no offset between the mean observed and generated sample completeness values at low redshifts, and at higher redshifts there is in fact a 6 per cent increase. The lack of a decrement here is a result of a number of non-selected quasars being particularly close to selection boundary, even though overall there are more quasars blue-ward of the cut-off.

To compare this with the current assessed level of completeness for $0.3 < z < 2.2$ objects in the 2QZ, the four non-stellar classified quasar discussed in Section 4.1 need to be taken into account, given that the 2QZ does not observe such objects. As all these objects are within the Ub_jR pre-selection region, this brings the assessed completeness level for the 2QZ pre-selection technique to 84 per cent. This is lower than the existing assessed

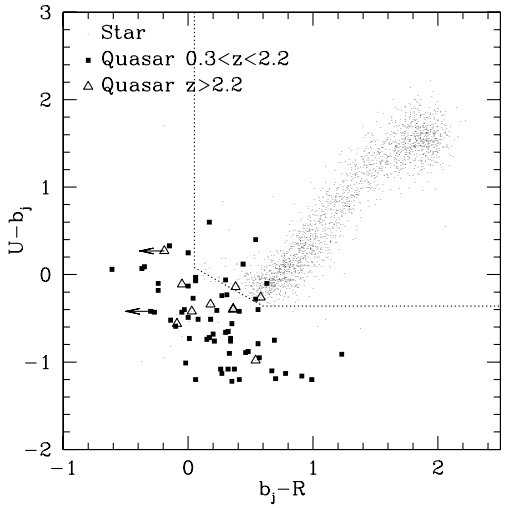

Figure 8. Ub_jR multicolour diagram showing colour pre-selection cut-off as currently being used in the 2QZ. Cut-off is given by $U - b_j \leqslant -0.36$, $U - b_j < 0.12 - 0.8(b_j - R)$, $b_j - R < 0.05$. Two quasars in the sample have magnitudes too faint to appear in the APM R-plate and as such are plotted with arrows and a location corresponding to an upper magnitude limit of $R = 20.3$.

level of >90 per cent (Croom et al. 1998). With the caveat that the Fornax survey has a brighter magnitude limit than that of the 2QZ, the results presented here, although lower than the stated completeness levels of the 2QZ, nevertheless confirm that the multicolour pre-selection criteria applied should achieve relatively high levels of completeness, but will still not find all the potentially observable quasars.

Our results could also be used to determine a new multicolour selection criterion for stellar sources which could detect all quasars. One such criterion is the L shaped cut-off $U - b_j < -0.36$ (as above) OR $b_j - R < 0.65$. Given that such a criterion includes part of the stellar locus, the number of unresolved quasars observed as a percentage of total stellar objects in the selected region is fairly low at 23 per cent. This compares to a percentage of 71 per cent for the Croom et al. (1998) selection criterion as similarly determined from the FSS data.

Given the apparent completeness differences between the UVX and multicolour pre-selection techniques, with 90^{+3}_{-4} per cent of low-redshift quasars being detected using the multicolour criterion as compared to 69 ± 6 per cent using UVX alone, it would be expected that there would be a corresponding difference in the quasar number counts obtained in the Durham/AAT survey compared to the 2QZ. This is not the case, however, with the number densities in fact being higher for the Durham/AAT survey at the magnitude limit examined. We are unaware of an explanation for this discrepancy.

4.4 The nature of quasars not detected by multicolour selection

Although not as many objects are missed by the Ub_jR 2QZ pre-selection technique as implied by the number counts in Section 3.1, 11 per cent of objects are still outside the pre-selection boundaries. It is therefore of interest to investigate the nature of these missed objects. In particular, of the eight non-selected quasars, we examine the six quasars at redshifts $0.3 < z < 2.2$ (numbers 4, 5, 17, 31, 58 and 61), looking for factors which may contribute to their unusual colours.

To begin with, we examined the non-Ub_jR detected quasars in terms of image morphology, absolute magnitude and z to see if there are any trends in the location of the non-selected quasars.

The lack of a morphological bias in the Fornax survey, with all objects being surveyed rather than just those classified as stellar, is a potentially important factor as it is low-luminosity, low-redshift objects that are more likely to have their host galaxies visible and hence be classified as non-stellar. However, in practice the objects classified as non-stellar by APM in the b_j band are all selected by the Ub_jR method as discussed in Section 4.3.

Examining the absolute magnitudes of non-selected objects, there is no particular trend, the non-selected objects being spread across the whole of the luminosity function. Similarly, comparing the redshifts of the non-selected quasars with the selected population using a Kolmogorov–Smirnov test, no significant difference is found at the 73 per cent level.

There are (at least) five potential causes for the redder colours of the non-selected quasars: first, the effects of contamination by objects along the line of sight or photographic plate defects; secondly, the effects of spectral features in particular passbands; thirdly, dust extinction; fourthly, variability; and lastly, intrinsically red continuum.

With respect to the first of these, film copies of the b_j and R photographic plates used in determining the APM magnitudes were examined for potential non-intrinsic influences on object colour. Of the $0.3 < z < 2.2$ non-selected objects, five are found to be clear measurements, with the objects being point sources and free from line of sight contamination. For quasar 17, there is a possibility that a diffraction spike from a nearby star along the line of sight may be infringing on the image of the quasar and hence affecting its colour. This spike is visible in both the b_j and R-plates, but it is unclear to what extent this may be affecting magnitude measurements. The magnitude of the diffraction spike is not such that it is registered in the digital interpretation of the plate by APM.

Secondly, the spectra of the six quasars were examined (see Appendix) for any strong emission lines or other features that might cause their unusual colours. No features were found, indicating that their colours are due to unusual continuum shapes. (Note that our 2dF spectra are not flux calibrated, so the shape of the continua cannot be directly measured).

In terms of continuum effects, intrinsic dust extinction is a plausible explanation for the unusual colours of these objects (Webster et al. 1995). Fig. 9 shows the two-colour plot for all the selected quasars within 0.6 in redshift of each of the six targets. Using standard reddening laws relating dust extinguished flux from an object (F'_λ) to unextinguished flux (F_λ):

$$F'_\lambda = F_\lambda e^{-\tau_\lambda}, \tag{2}$$

where the optical depth τ_λ is given by

$$\tau_\lambda = C\lambda^{-n}; \tag{3}$$

we can see that reddening by dust with a scale factor n=1 and a plausible extinction in the rest V-band of $A_V = 0.75$ mag (Masci, Drinkwater & Webster 1999) *can* shift the 'missing' quasars into the usually selected region of the plot. Quasars 5 and 17, however, would still be at or close to the red edge of the distribution in $U - b_j$, and a smaller extinction for quasars 61 would bring it closer to the quasar locus. Dust extinction may also be occurring

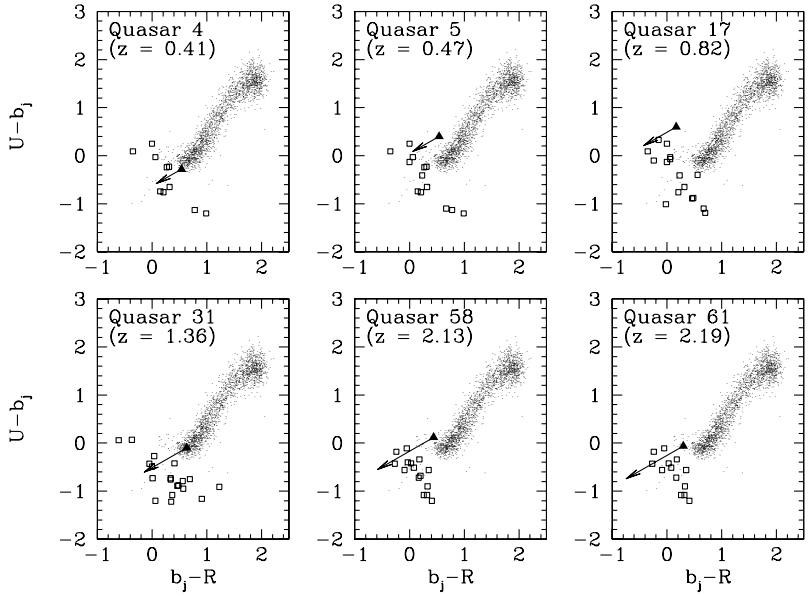

Figure 9. Non-multicolour selected $0.3 < z < 2.2$ quasars (triangles) plotted with other quasars in a 0.6 redshift bin centred on the non-selected quasar (squares). Also plotted are APM stellar objects observed in the survey. The arrows drawn are reddening vectors using standard dust extinction laws with $n = 1$ and $A_V = 0.75$ mag.

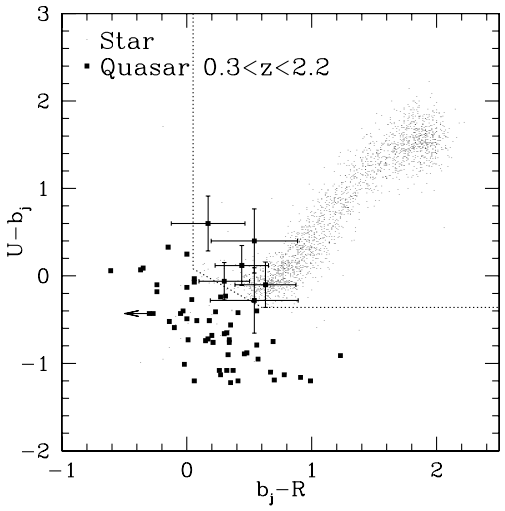

Figure 10. Potential effects of variability on non-multicolour selected $0.3 < z < 2.2$ quasar colours. Errors are determined using variability parametrization of Hook et. al. (1994). Quasar data point with arrow was too faint to appear in the APM R catalogue, and its $b_j - R$ colour is based on an R-magnitude limit of 20.3.

at lower redshifts, however these effects are likely to be smaller (Masci et al. 1999).

Quasar variability is a potential effect in the red appearance of the non-selected objects as the APM plates used in the input catalogue are not contemporaneous (see Section 2.1). To gauge the potential effects of this, the variability parametrization of Hook et al. (1994) is used:

$$|\Delta m| = [0.155 + 0.023(M_B + 25.7)]\Delta t_{\rm rest}^{0.18} \quad (4)$$

where $\Delta t_{\rm rest} = \Delta t_{\rm obs}/(1+z)$ is the rest frame interval in between observations [$\Delta t_{\rm obs} = 21$ yr for $\sigma(U - b_j)$ and 15 yr for $\sigma(b_j - R)$]. Fig. 10 shows the corresponding colour errors. In taking the errors in each direction to be uncorrelated, these errors likely overestimate the real effects of variability. Of interest here is that although a potential contributing factor, variability cannot fully account for unusual colour of these objects. It should be noted that these variability effects will also apply to any survey using non-contemporaneous input catalogue plates to preselect quasar candidates, e.g. 2QZ.

Table 4. Completeness levels for ultraviolet excess and multicolour pre-selection techniques obtained from Fornax Spectroscopic Survey data.

Technique	Redshift	Completeness (per cent)
UVX	$0.3 < z < 2.2$	69 ± 6
	$z > 2.2$	50^{+14}_{-18}
Multicolour	$0.3 < z < 2.2$	90^{+3}_{-4}
	$z > 2.2$	80^{+14}_{-12}

5 CONCLUSIONS

Utilizing the 2dF multi-object spectrograph on the AAT, we have, as part of the much larger Fornax Spectroscopic Survey, conducted the first spectroscopically complete quasar survey of a significant area of sky. In the FSS to date, the spectra of 3679 astrophysical objects have been successfully identified, with 71 quasars found in the π-deg^2 area. As well as providing a new determination of quasar number counts, this has for the first time provided an independent check of the completeness levels of existing surveys. These number count comparisons indicate incompleteness in surveys utilizing traditional pre-selection techniques, however 2-sigma errors on our numbers cannot rule out 100 per cent completeness in most cases. Given the availability of U, b_j and R magnitudes from the input catalogue, however, an independent examination is made of UVX and multicolour pre-selection techniques. This indicates that the use of

$U - b_j$ colour alone *does* fail to select a significant proportion of quasars, with completeness values of 69 ± 6 per cent for $0.3 < z < 2.2$ quasars and 50^{+14}_{-18} per cent for $z > 2.2$ quasars. The addition of a second colour, $b_j - R$, although significantly increasing the completeness levels for quasar selection to 90^{+3}_{-4} per cent for $0.3 < z < 2.2$ quasars and 80^{+14}_{-12} per cent for $z > 2.2$ quasars, is again nevertheless found not to detect all quasars.

We further note that as 7 per cent of the low-redshift FSS quasars are non-stellar on the basis of image classification, these figures are bound to decrease for surveys only examining stellar objects.

Investigating the nature of the remaining multicolour non-selected objects, we find that all are point sources, with insignificant host galaxy contribution to their colour. Taking the non-selected $0.3 < z < 2.2$ quasars, with the possible exception of quasar 17, the colours of these objects appear not to be due to any image confusion on photographic plates. If intrinsic, their colours are most likely to be the result of unusual continua rather than emission line effects, with intrinsic dust extinction being a possible cause. Variability was examined as a potential cause of their unusual colour, however was found to be unable to fully account for this.

To increase the statistical significance of the results obtained, we require as a first step, observations of the remaining $16.5 < b_j < 20.0$ input catalogue objects not yet successfully identified, as well as contemporaneous colour measurements. In the longer term, the significance will be greatly enhanced by the continuation of the survey into FSS fields 2, 3 and 4.

ACKNOWLEDGMENTS

We would like to thank the referee Scott Croom for his many useful comments which helped us improve the presentation of this paper. The FSS would not have been possible without the development of 2dF at the AAO and the allocation of time by PATT and ATAC to the FSS as a bi-national project. The UKSTU is thanked for supplying the plates used to construct the catalogues, and the APM group for scanning the plates. MJM and MJD acknowledge the support of the University of Melbourne and the Australian Research Council, respectively. Much of the work was carried out while SP was supported by the Royal Society via a University Research Fellowship. WJC acknowledges the hospitality of the University of Bristol, the University of St Andrews and the European Southern Observatory during the course of this work.

REFERENCES

Boyle B. J., Fong R., Shanks T., Peterson B. A., 1990, MNRAS, 243, 1
Boyle B. J., Croom S. M., Smith R. J., Shanks T., Miller L., Loaring N., 1999, Phil. Trans. R. Soc. Lond. A, 357, 185
Boyle B. J., Shanks T., Croom S. M., Smith R. J., Miller L., Loaring N., Heymans C., 2000, MNRAS, 317, 1014
Crampton D., Cowley A. P., Hartwick F. D. A., 1987, ApJ, 314, 129
Croom S. M., 1997, PhD thesis, Univ. Durham
Croom S. M., Shanks T., Boyle B. J., Smith R. J., Miller L., Loaring N. S., 1998, Evolution of Large-Scale Structure: From Recombination to Garching. In press (astro-ph/9810127) (E32)
Drinkwater M. J. et al., 2000, A&A, 355, 900 (Paper I)
Francis P., 1991, ApJ, 373, 465
Graham M. J., Clowes R. G., Campusano L. E., 1999, ApJ, 513, 69
Hagan H. J., Groote D., Engels D., Reimers D., 1995, A&AS, 111, 195
Hartwick D., Schade D., 1990, ARA&A, 28, 437
Hawkins M. R. S., Veron P., 1995, MNRAS, 275, 1102
Hewett P. C., Foltz C. B., 1994, PASP, 106, 113
Hewett P. C., Foltz C. B., Chaffee F. H., 1995, AJ, 109, 1498
Hewitt A., Burbidge G., 1993, ApJS, 87, 451
Hilker M., Infante L., Vieira G., Kissler-Patig M., Richtler T., 1999, A&AS, 134, 75
Hook I. M., McMahon R. G., Boyle B. J., Irwin M. J., 1994, MNRAS, 268, 305
Irwin M. J., Maddox S., McMahon R., 1994, Spectrum, 2, 14
Koo D., Kron ., Cudworth K., 1986, PASP, 98, 285
La Franca F., Cristiani S., 1997, AJ, 113, 5
Masci F. J., Drinkwater M. J., Webster R. L., 1999, ApJ, 510, 703
Newberg H. J., Yanny B., 1997, ApJS, 113, 89
Osmer P. S., Kennefick J. D., Hall P. B., Green R. F., 1998, ApJS, 119, 189
Schlegel D. J., Finkbeiner D. P., Davis M., 1998, ApJ, 500, 525
Smith R. J., Boyle B. J., Shanks T., Croom S. M., Miller L., Read M., 1997, in McLean B. J., Golombek D. A., Hayes J. J. E., Payne E., eds, Proc. IAU Symp. 179, New Horizons from Multi-Wavelength Sky Surveys. Kluwer, Dordrecht, p. 348
Smith R. J., 1998, PhD thesis, Univ. Cambridge
Tonry J., Davis M., 1979, AJ, 84, 10
Warren S. J., Hewett P. C., Irwin M. J., Osmer P. S., 1991, ApJS, 76, 1
Webster R. L., Francis P. J., Peterson B. A., Drinkwater M. J., Masci F. J., 1995, Nat, 375, 469
Wisotzki L., Köhler T., Groote D., Reimers D., 1996, A&AS, 115, 227
Zitelli V., Mignoli M., Zamorani G., Marano B., Boyle B., 1992, MNRAS, 256, 349

APPENDIX A: QUASAR SPECTRA

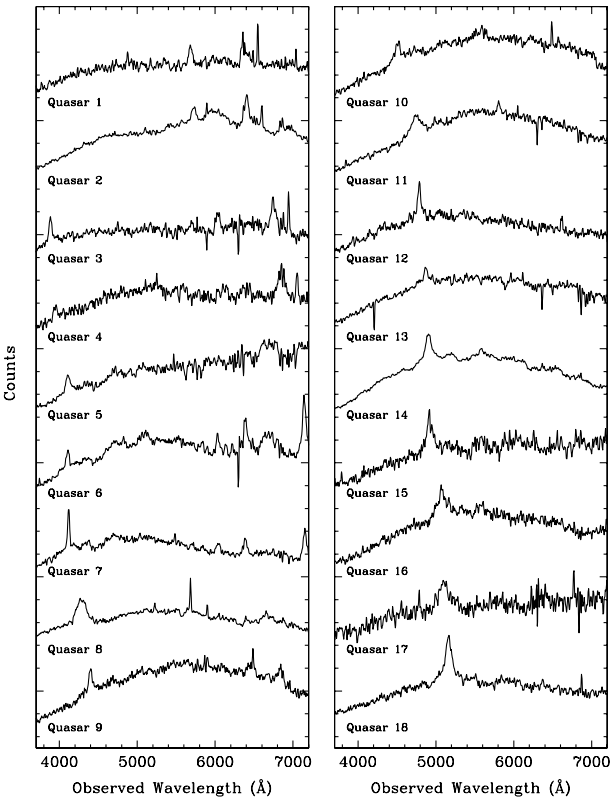

Figure A1. Spectra for Quasars 1–18.

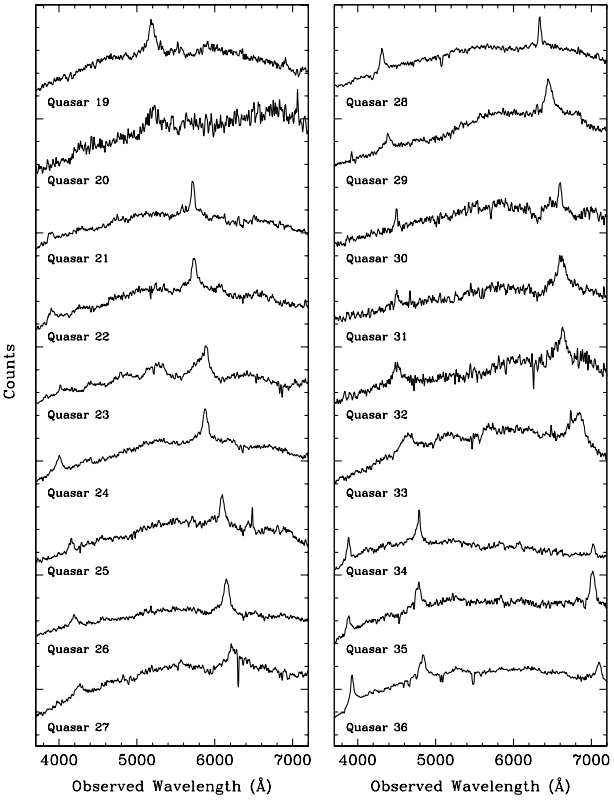

Figure A2. Spectra for Quasars 19–36.

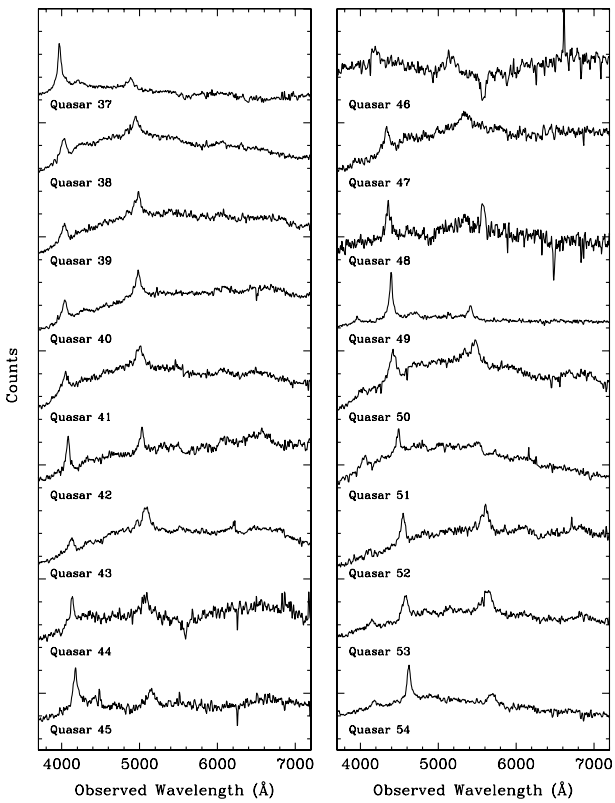

Figure A3. Spectra for Quasars 37–54.

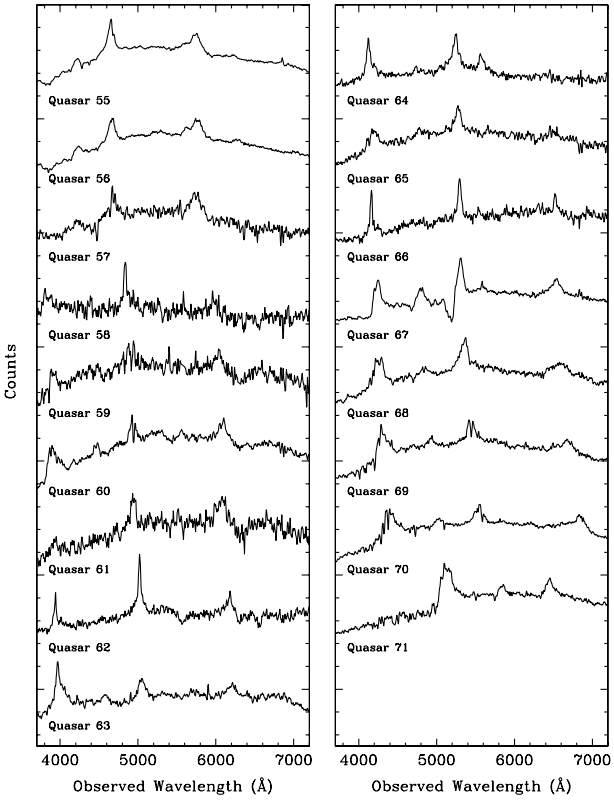

Figure A4. Spectra for Quasars 55–71.

This paper has been typeset from a TEX/LATEX file prepared by the author.